Vacuum 120 (2015) 116–120

Contents lists available at ScienceDirect

Vacuum

journal homepage: www.elsevier.com/locate/vacuum

Short communication

Thermo-hydrodynamic process simulation of craters formation and evolution on metal surfaces caused by intense pulsed ion beams

Xiao Yu [a], Jie Shen [a], Haowen Zhong [a], Jie Zhang [a], Sha Yan [b], Gaolong Zhang [a], Xiaofu Zhang [a], Xiaoyun Le [a, *]

[a] School of Physics and Nuclear Energy Engineering, Beihang University, Beijing 100191, PR China
[b] Institute of Heavy Ion Physics, Peking University, Beijing 100871, PR China

ARTICLE INFO

Article history:
Received 10 April 2015
Received in revised form
3 June 2015
Accepted 18 June 2015
Available online 26 June 2015

Keywords:
Intense pulsed ion beam
Crater
Surface tension
Level-set method

ABSTRACT

As observed in many studies, craters may appear on the surfaces of metals after irradiation of intense pulsed ion beams (IPIB). These craters limit the utilization of IPIB as a novel method for surface processing in some cases. In this work, taking stainless steel as an example, the hydrodynamic behavior of molten surface formed by IPIB was taken into consideration, by taking IPIB-induced heat transfer and level-set method flow field analysis with finite element method (FEM) we deduced that prior temperature rise by the thermal resistance of grain boundary is the causes of craters. For metals and alloys with relatively higher viscosity and surface tension, the uneven distribution in the curvature and stress in the molten surface leads to the mass redistribution and the flattening trend in the surface morphology.

Intense pulsed ion beam (IPIB) has been drawing more and more attention as a novel means of surface processing. It was utilized for various surface treating applications such as surface hardening, wear and corrosion resistance improving, crack healing, fine graining, and so on [1–3]. As observed in many studies, μm-sized craters may be created during IPIB irradiation and this may lead to catastrophic deterioration in severing properties of the irradiated parts [4]. As a result, it is of great significance to study the crater formation and evolution mechanism in order to minimize the negative effect of craters.

In the past two decades, quite a lot of efforts have been paid to the formation mechanism of craters. Experimental research has been carried out on materials such as steel [5], copper [6], silicon [6], titanium [7] and its alloys [8], etc. and the relationship between IPIB parameters (ion energy, beam density, pulsed number, etc.) and crater features (such as shape, size and distribution) were intensively studied in these researches. Quite a lot of empirical knowledge was obtained about the creation conditions of craters. Based on the summarizing of experimental research, some trials have been made to give theoretical explanations of the formation mechanism of craters.

As have been demonstrated, much fewer craters were found on single crystal material targets, such as the case of copper and silicon after IPIB irradiation [6] and it was concluded that the grain structure affects cratering. In order to clarify the origin of cratering, theoretical analysis was carried out focusing on the ion-induced vacancies [9]: vacancy clusters may be generated during ion injection and the gathered vacancy clusters grow up to bigger voids which finally acts as the crater erupting centers. Grain boundaries were considered as bases of void formation and short-cuts of small pores. Some attempts took the IPIB-induced thermal stress into consideration and attributed the formation of craters to the lateral confinement of thermal stress [10]. These theories can explain some experimental results, however, a major limitation of these models is that they did not take the melting surface state into account and thus theories in solid state were used for the phenomena actually in the liquid state. This leads to difficulties in explaining mass transportation caused by IPIB.

In order to perform the hydrodynamic analysis, a thermal conduction analysis was taken first to estimate the temporal and spatial features of the flow field. As the cross-sectional size of IPIBs are typically in tens of cm, much larger compared with the ranges of ions in solid target (for typical apparatus [1–3], energy of ions are within 1 MeV and the ranges in solid targets are within several μm), so taking 1-D approximation is reasonable. The 1-D thermal field evolution simulation of IPIB with cross-sectional energy density of

* Corresponding author.
E-mail address: xyle@buaa.edu.cn (X. Le).

http://dx.doi.org/10.1016/j.vacuum.2015.06.028
0042-207X/

1 and 3 J/cm^2 in 304 stainless steel was carried out. The Fourier thermal condition equation was adopted as the governing equation:

$$\rho C_V \frac{\partial T}{\partial t} = \lambda \nabla^2 T + P \tag{1}$$

where ρ, C_V, and λ are the density, specific heat and thermal conductivity of the target, respectively. For $P(z, t)$, we used the method and model to define the source term mentioned in Ref. [11]: the form of P was approximated as:

$$P(x, y, z, t) = U(x, y) \cdot d(z) \cdot g(t) \tag{2}$$

In which, $P(x, y, z, t)$ is the beam power density distribution on the target; $U(x, y)$ is the beam energy distribution function along the x-y plane, i.e., on the cross section of the beam, and can be measured by energy diagnostic method such as calorimeters and infrared diagnostics. In one-dimensional case, $U(x, y)$ is a constant; $d(z)$ is the depth-normalized energy loss distribution vs. the depth z, and can be deduced from the particle stopping power dE/dz, in this study it is calculated with Monte Carlo codes SRIM [12]; $g(t)$ is the time-normalized power evolution function, which can be estimated from the IPIB current density acquired by Faraday cup. In this study, we took IPIB parameters from pulsed accelerator BIPPAB-450 composed mainly of protons with maximum ion energy of 450 keV. For initial condition we take

$$T(z, 0) = T_0 \tag{3}$$

where T_0 is 298 K.

For boundary condition, in order to evaluate the energy loss by infrared radiation, Stefan–Boltzmann boundary condition was taken:

$$j = \varepsilon\sigma\left(T^4 - T_0^4\right) \tag{4}$$

in which j is the surface-to-ambient radiative heat flux, σ is the Stefan–Boltzmann constant, ε is the emissivity and $\varepsilon = 0.3$. The equation is solved by the finite element method (FEM) software Comsol Multiphysics.

Fig. 1 demonstrates the temperature field induced by IPIB in stainless steel. As can be observed, for 1 J/cm^2 IPIB, the highest temperature is lower than 1500 K, even lower than the melting point of stainless steel, the flowing of the surface cannot be formed and for the surface, no obvious mass transportation can be observed. Also, under this condition, the viscosity of the molten metal is considerably large. The temperature-related fluidity of the liquid is rather poor and this greatly limits the moving of the surface. For IPIB with energy density of 3 J/cm^2, by making the intersecting line between the temperature distribution surface and melting point plane (the highlighted red curve in Fig. 1. b) it is demonstrated that within a depth of over 3 μm the target can be in liquid state; in the target within a depth of 2.5 μm, the liquid state can exist for a period of almost 500 ns. This signifies that, for every IPIB pulse, for a depth of within 2 μm, for a time scale of several hundred ns, the state of the target can be described with hydro-approximation. Note that as the energy deposition of IPIB along the depth of the target is dominated by the range of the ions, under the same cross-sectional energy density, IPIB with shorter ion ranges, such as the IPIB composed mainly by carbon ions and lower ion energy (<250 keV) generated by accelerator TEMP-4M [13] induces much stronger thermal effects on the near-surface region and this may leads more obvious hydrodynamic effects.

Also, for 3 J/cm^2 IPIB, the maximum temperature in the target is far above the evaporating point of the target and this gives rise to

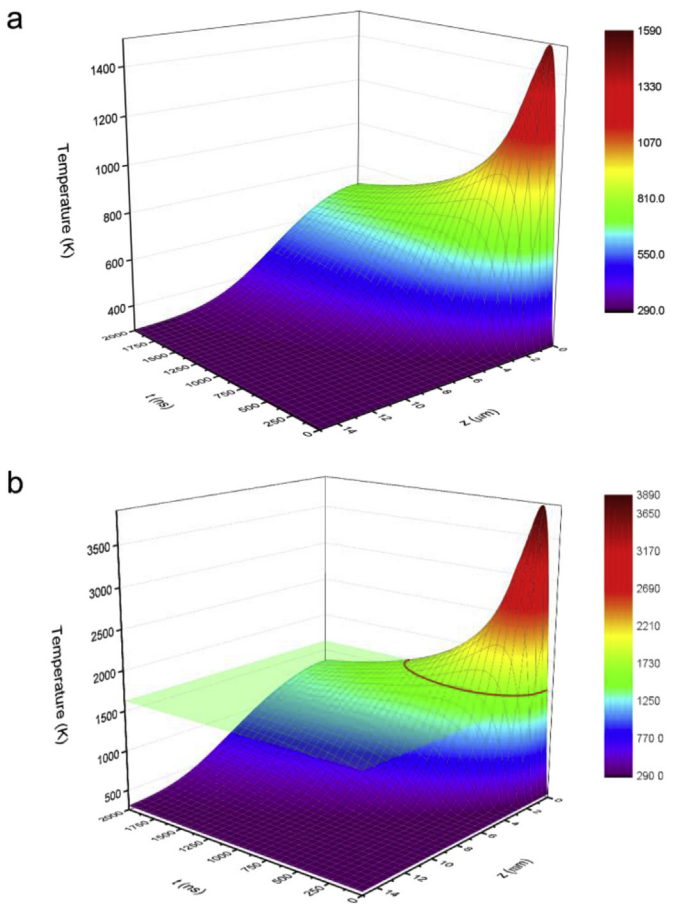

Fig. 1. Temperature field induced by IPIB with cross-sectional energy density of 1 J/cm^2 (a) and 3 J/cm^2 (b) in 304 stainless steel.

ablation gas formation and ejection. In previous studies, it was taken that the Bragg-peak effect of the ion beam can lead to a prior ejection under the surface [7]. However, by time-of-flight analysis it is revealed that as a consequence of the over-lapping effect of ions with various energies, the surface of the target tends to reach the evaporating point first [11,13]. Here we attribute the formation of ejecting craters to the thermal resistance change formed by grain boundary. As a rise in thermal resistance can be formed by the grain boundary, temperature can make a prior rise in this position. Some experimental results can be explained by this such as the randomness of crater formation and distribution on the target surface; different cratering behavior on single and poly crystal targets; the feature sizes of craters are on the same order with grain sizes.

For hydrodynamic analysis of the molten surface, level-set method [14] was used to track the interface between molten metal and high-vacuum surrounding gas. The flow of the liquid and the gas were modeled with the Navier–Stokes (N–S) equations for incompressible laminar flow:

$$\rho \frac{\partial \boldsymbol{u}}{\partial t} - \nabla \cdot \mu\left(\nabla \boldsymbol{u} + (\nabla \boldsymbol{u})^T\right) + \rho(\boldsymbol{u} \cdot \nabla)\boldsymbol{u} + \nabla p = \boldsymbol{F} \tag{5}$$

$$\nabla \cdot \boldsymbol{u} = 0 \tag{6}$$

where ρ is the density of fluid, $\boldsymbol{u}$ is the flow velocity vector, μ is the dynamic viscosity, p is the pressure, $\boldsymbol{F}$ is the source term, in this case it is imposed by the surface tension at the liquid–gas interface.